J Mater Sci (2011) 46:365–371
DOI 10.1007/s10853-010-4843-3

The effects of calcium and yttrium additions on the microstructure, mechanical properties and biocompatibility of biodegradable magnesium alloys

Yuncang Li · Peter D. Hodgson · Cui'e Wen

Received: 20 June 2010 / Accepted: 14 August 2010 / Published online: 2 September 2010

Abstract In this study, the effects of calcium (Ca) and yttrium (Y) on the microstructure, mechanical properties, corrosion behaviour and biocompatibility of magnesium (Mg) alloys, i.e. Mg–*x*Ca ($x = 0.5$, 1.0, 2.0, 5.0, 10.0, 15.0 and 20.0%, wt%, hereafter) and Mg–1Ca–1Y, were investigated. Optical microscopy, X-ray diffractometry (XRD), compressive and Vickers hardness testing were used for the characterisation and evaluation of the microstructure and mechanical properties. The in vitro cytotoxicity of the alloys was assessed using osteoblast-like SaOS2 cells. The corrosion behaviour of these alloys was evaluated by soaking the alloys in simulated body fluid (SBF) and modified minimum essential medium (MMEM) at 37 °C in a humidified atmosphere with 5% CO_2. Results indicated that the increase of the Ca content enhances the compressive strength, elastic modulus and hardness of the Mg–Ca alloys, but deteriorates the ductility, corrosion resistance and biocompatibility of the Mg–Ca alloys. The Y addition leads to an increase in the ductility; but a decrease in the compressive strength, hardness, corrosion resistance and biocompatibility of the Mg–1Ca–1Y alloy when compared to the Mg–1Ca alloy. Solutions of SBF and MMEM with the immersion of Mg–*x*Ca and Mg–1Ca–1Y alloys show strong alkalisation. Our research results indicate that Mg–*x*Ca alloys with Ca additions less than 1.0 wt% exhibited good biocompatibility, low corrosion rate as well as appropriate elastic modulus and strength; whilst the Y is not a proper element for Mg alloys for biomedical application due to its negative effects to the corrosion resistance and biocompatibility.

Y. Li (✉) · P. D. Hodgson · C. Wen
Institute for Technology Research and Innovation, Deakin University, Geelong, VIC 3217, Australia
e-mail: yuncang.li@deakin.edu.au

Introduction

Magnesium (Mg) alloys have attracted widespread attention as new biodegradable implant materials for potential applications in orthopaedics [1–5]. Mg is a natural ionic presence with significant functional roles in biological systems and bone tissue [6–9] and may actually have stimulatory effects on the growth of new bone tissue [4, 5, 10, 11]. Mg and its alloys are light and mechanical properties similar to natural bone [1]. The elastic modulus and compressive yield strength of Mg are closer to those of natural bone than in the case for other commonly used metallic implants [1, 12–18]. Mg and its alloys are biodegradable in aqueous solution, particularly in those containing chloride electrodes. These promising characteristics have inspired the researchers to develop Mg and its alloys to serve as biocompatible, osteoconductive and biodegradable implants [3, 19–26]. However, pure Mg may degrade too quickly in the physiological system, producing hydrogen gas in the corrosion process and leading to lose mechanical integrity before the tissue has sufficiently healed. Moreover, pure Mg possesses poor mechanical performance [1, 10, 13, 16, 24].

To improve the mechanical strength and corrosion resistance of pure Mg, one way is to alloying by using biocompatible alloying elements [27–29]. It has been reported that calcium (Ca) and yttrium (Y) are favourable non-toxic metals [30, 31]. Furthermore, it has been reported that the alloying addition of Ca can increase the mechanical property and corrosion resistance of Mg alloys significantly [32]. Dabah et al. [33] reported that increasing the Ca content from 0.9 to 1.8 wt% improves the corrosion resistance of the alloy; Ca addition causes a reduction of the average grain size, which increases corrosion resistance as the precipitates located at grain boundaries are more

continuous and act as a barrier to the advance of corrosion. Aghion and Levy [34] also found that the addition of 0.4% Ca has a beneficial effect on the corrosion resistance of the Mg–1.2%Nd–0.5%Y–0.5%Zr alloy. New Mg alloys with the addition of rare earth element Y demonstrated slowed corrosion rate [35–37]. Ca is a very important element in the human body and 99% or more of the Ca is deposited in bone and the remainder is importantly associated with nerve conduction, muscle contraction, hormone release and cell signalling [38]. Ca is an important Mg alloying element that affects the mechanical property and corrosion resistance significantly [32].

In this study, to evaluate the effects of Ca and Y on the mechanical properties, the corrosion behaviour and the cytotoxicity of Mg alloys, Mg–*x*Ca alloys ($x = 0.5$, 1, 2, 5, 10, 15 and 20.0) and Mg–1Ca–1Y alloy were prepared by a casting method. The microstructure and mechanical properties of the Mg–*x*Ca alloys and Mg–1Ca–1Y alloy were investigated. The in vitro cytotoxicity was assessed using osteoblast-like SaOS2 cells. The corrosion behaviour of the Mg alloys in simulated body fluid (SBF) and modified minimum essential medium (MMEM) was evaluated.

Experimental and methods

Preparation of the Mg alloy samples

The Mg–*x*Ca and Mg–1Ca–1Y alloys were prepared by casting from the melt of pure Mg, Ca and Y under an atmosphere of pure argon using a steel crucible. Disc samples with a diameter of 9 mm and thickness of 2 mm were cut from the ingot for structure characterisation and in vitro cell culture study. Cylindrical samples with a diameter of 5 mm and height of 10 mm were cut from the ingot for the compressive test.

Microstructure characterisation and mechanical property testing

Characterisation of the microstructure and phases of the Mg alloys was carried out using optical microscope and X-Ray Diffractometer (XRD), respectively. To evaluate the mechanical properties, compressive tests were carried out at room temperature and an initial strain rate of 10^{-3} s^{-1} using an Instron universal test machine equipped with a video extensometer (Instron 5567, USA).

Immersion testing

The immersion testings were carried out by soaking in SBF and MMEM at 37 °C in a humidified atmosphere with 5% CO_2 according to ASTM-G31-72 [39]. The SBF was prepared by dissolving the following chemicals in sequence: NaCl (5.403 g), $NaHCO_3$ (0.504 g), Na_2CO_3 (0.426 g), KCl (0.225 g), $K_2HPO_4{\cdot}3H_2O$ (0.230 g), $MgCl_2{\cdot}6H_2O$ (0.311 g), $CaCl_2$ (0.293 g) and Na_2SO_4 (0.072 g). The solution was buffered to pH 7.40 with HEPES and 1 M NaOH at 37 °C [40]. The MMEM contained minimum essential media (MEM) (Gibco, Invitrogen, Australia) supplemented with 10% fetal bovine serum (Bovogen Biologicals, Melbourne, Victoria, Australia), 1% non-essential amino acid (Sigma-Aldrich, Castle Hill, New South Wales, Australia), 10,000 units/mL penicillin–10,000 μg/mL streptomycin (Gibco, Invitrogen, Australia) and 0.4% amphostat B (Invitro, New Zealand).

After immersion, the samples were removed from SBF and MMEM, gently rinsed with distilled water, washed by CrO_3 and dried at room temperature. The corrosion rate was calculated by the weight loss. The pH value of the SBF and the modified media was monitored during the soaking. An average of five measurements was taken for each group.

Cytotoxicity assessment

SaOS2 osteoblast-like cells were cultured in MMEN at 37 °C in a humidified atmosphere with 5% CO_2. The cytotoxicity tests were carried out by indirect contact according to ISO 10993-5 [41]. The control groups involved the use of MMEM as negative controls. Cells were incubated in 48-well cell culture plates at 3,000 cells/300 μL media/well and incubated for 24 h to allow attachment. The media was then replaced with 150 μL of extracts. After 24 h incubating, cells were harvested using 0.1% Trypsin-5 mM EDTA (Sigma-Alrdrich, Australia) and collected. Cell counts were obtained using the trypan blue exclusion method [42], whereby dead cells were stained blue and live cells remained clear. The cell viability was determined by the ratio of live cells to the total number of cells per sample. The viability of the cell on the Mg alloys is defined as the ratio of the live cell number to total cell number (live cell plus dead cell) in extraction media.

Results and discussion

Mechanical properties of the Mg–Ca alloys

The results of compressive and hardness tests were shown in Fig. 1. It can be seen that the elastic modulus, compressive strength and Vickers hardness of the Mg–*x*Ca alloys increase with the increasing Ca content (Fig. 1a and b). The elastic modulus of the Mg–*x*Ca alloys increases from 15.0 GPa for the Mg–0.5Ca to 34.8 GPa for the Mg–20Ca. The compressive strength of the Mg–*x*Ca alloys increases from 160 MPa for the Mg–0.5Ca to 300 MPa for the Mg–20Ca.

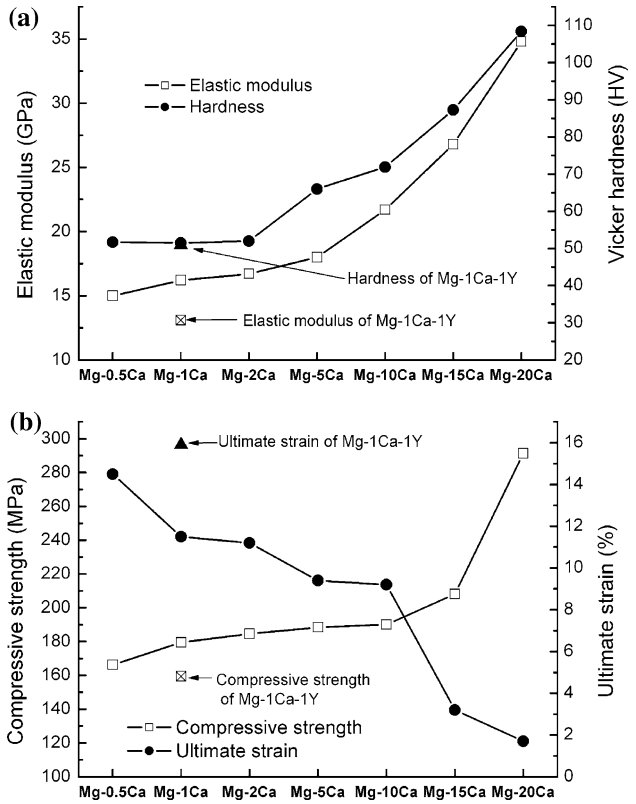

Fig. 1 **a** Elastic modulus and hardness and **b** compressive strength and ultimate strain of Mg–*x*Ca and Mg–1Ca–1Y alloys

Similarly, the elastic modulus increases from 15 to 30 GPa, and the Vickers hardness increases from 18 to 110 HV for the lowest Ca content (0.5 wt%) and the highest Ca content (20.0 wt%), respectively. However, the ultimate strain decreases with the increasing of Ca content in the Mg–Ca alloys (Fig. 1b), which indicates that the Mg–*x*Ca alloy becomes brittle with the increasing level of Ca content. It should be noted that the ductility (ultimate strain) of the Mg–*x*Ca alloy decreases with the increase of Ca content (Fig. 1b). Kim et al. [43] also reported the similar results that the Ca element generally increased the flow strength and decreased the ductility of AZ31 alloy at low temperature.

The elastic modulus of Mg–1Ca–1Y alloy is 13.1 GPa and a little lower than 16.2 GPa of the Mg–1Ca alloy (Fig. 1a). The compressive strength of Mg–1Ca–1Y alloy is 159.4 MPa compared to 179.8 MPa of the Mg–1Ca alloy (Fig. 1b). There is no significant difference between the hardness for the Mg–1Ca and the Mg–1Ca–1Y alloys. Moreover, the ultimate strain increases to 15.9% from 13.1% with the 1% addition of Y content in the Mg–1Ca alloy (Fig. 1b). It can be summarised that the Y addition improves the ductility of the Mg–*x*Ca alloys.

It has been reported that the compressive strength of the natural bone is in the range of 30–323 MPa, the elastic modulus ranges from 0.1 to 30 GPa and the hardness ranges from 16 to 168 HV [12–14]. The compressive strength (160–300 MPa), the elastic modulus (15–30 GPa) and hardness (18–110 HV) of the Mg–*x*Ca alloys are very close to those of natural bone.

Microstructure of the Mg–*x*Ca and Mg–1Ca–1Y alloys

Figure 2 shows the microstructures of the Mg–*x*Ca and Mg–1Ca–1Y alloys, and Fig. 3 shows the XRD patterns of the Mg–*x*Ca alloys. It can be seen that the microstructure varies with the amount of Ca additions. Mg_2Ca phase (as identified by XRD as shown in Fig. 3) precipitates along the Mg(α) primary grain boundaries of the Mg–*x*Ca and Mg–1Ca–1Y alloys. With increasing the addition level of Ca up to 15%, the morphology of the Mg alloy phase changed from spherical to petal-like. The grain size decreases, but the Mg_2Ca phase that distributes along Mg(α) primary grain boundaries increases with the increase of Ca content (as shown in Fig. 2a–f). It has been reported that Ca addition leads to the formation of a thermal stable second phase Mg_2Ca, which results in the grain refinement of Mg casting [44, 45]. Moreover, the room temperature ductility of Mg–Ca alloys is poor as Mg_2Ca is naturally brittle and precipitate preferentially at grain boundaries [46–48]. These phenomena are well reflected on the compressive tests. Pure Ca phase emerges in Mg–10Ca, Mg–15Ca and Mg–20Ca alloys. Mg–20Ca exhibits large grain size and a large amount of Ca phase (Figs. 2g, 3). It can also be seen that Y addition reduces the boundaries between Mg(α) primary grains and the Mg–1Ca–1Y alloy exhibited a more homogeneous microstructure than the Mg–1Ca alloy (Fig. 2b and h).

Corrosion behaviour of the Mg–*x*Ca and Mg–1Ca–1Y alloys

The corrosion rates for the Mg–(5–20)Ca alloys were not obtained since these alloys reacted with the SBF and MMEM solutions violently and broke into pieces quickly. Table 1 lists the corrosion rates of Mg–0.5Ca, Mg–1Ca, Mg–2Ca and Mg–1Ca–1Y alloys when soaking in SBF and MMEM at 37 °C in a humidified atmosphere with 5% CO_2. It can be seen that the corrosion rate of the Mg–*x*Ca alloys increases with the increase of Ca content. It should also be noted that the Mg–*x*Ca ($x = 0.5$, 1.0 and 2.0%) alloys degraded quicker in MMEM than in SBF. Meanwhile, Mg–1Ca–1Y shows a corrosion rate of 98.4 μg/mm^2/day in MMEM and 142.7 μg/mm^2/day in SBF when compared to the corrosion rate of 4.5 μg/mm^2/day in MMEM and 2.6 μg/mm^2/day in SBF for the Mg–1Ca alloy, respectively. The results indicate that the Y addition accelerates the corrosion of the Mg–1Ca alloy in both SBF and MMEM significantly. Figure 4 shows the pH values of the MMEM (a) and SBF (b) solutions varying with the

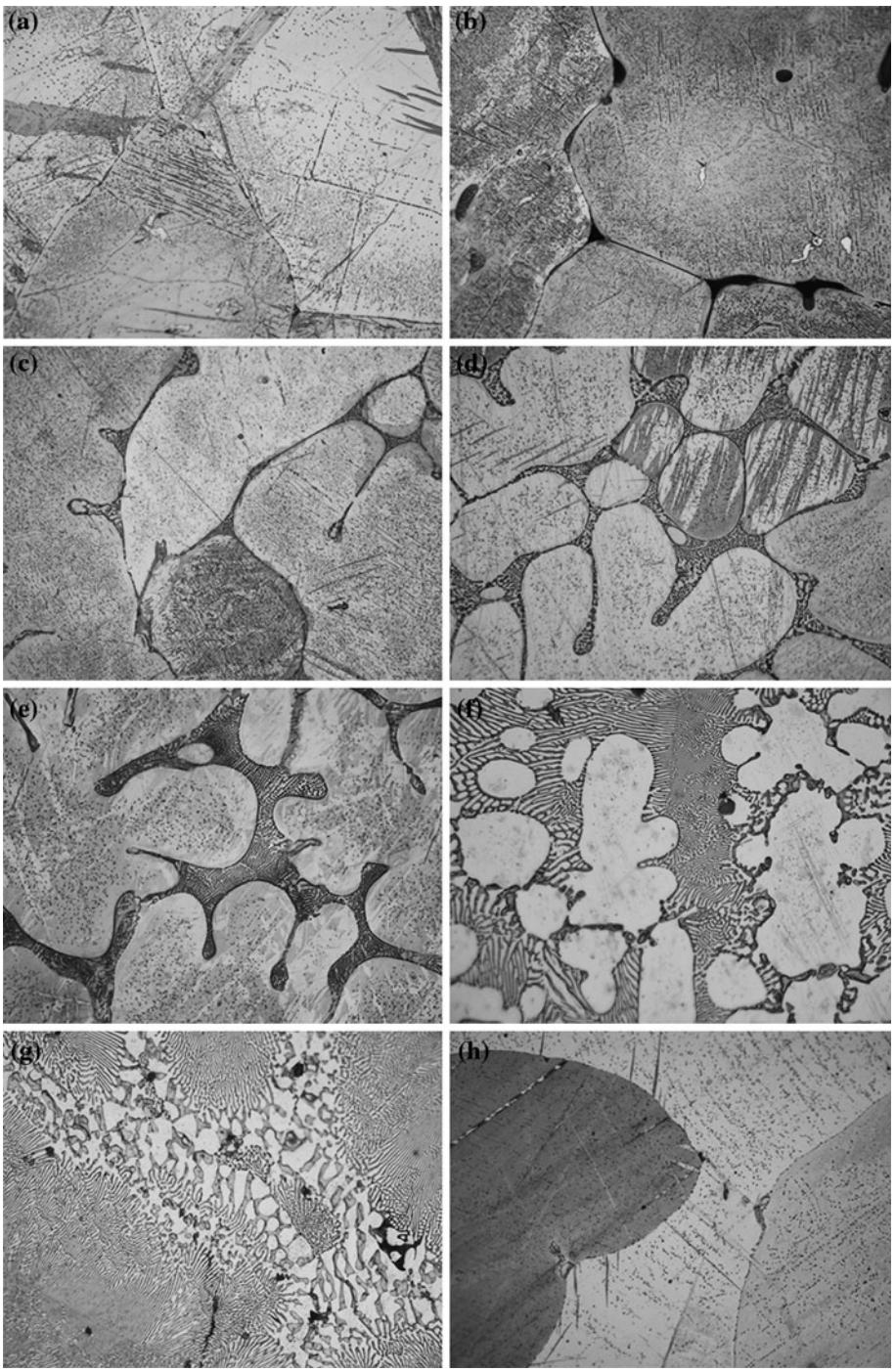

Fig. 2 Optical micrographs of **a** Mg–0.5Ca, **b** Mg–1Ca, **c** Mg–2Ca, **d** Mg–5Ca, **e** Mg–10Ca, **f** Mg–15Ca, **g** Mg–20Ca and **h** Mg–1Ca-1Y

immersion time of all the Mg alloys. It can be seen that the pH values of both the MMEM and SBF solutions increase rapidly with the immersion time from 9 to 20 h, and remained almost at the same level with prolonging the immersion time. The solutions of SBF and MMEM with the immersion of Mg alloys show strong alkalisation. It is also noticeable that the higher Ca content of the Mg alloys, the stronger alkalisation of the solutions of SBF and MMEM after the immersion of the Mg alloys (Fig. 4).

Cytotoxicity of the Mg–*x*Ca and Mg–1Ca–1Y alloys

As for the Mg–*x*Ca alloys with Ca content from 5.0 to 20.0%, similar to the corrosion behaviour as mentioned above, the cytotoxicity of the Mg–(5–20)Ca alloys was not obtained because these alloys reacted with MMEM violently and broke into pieces quickly. Figure 5 shows the cell viabilities of the SaOS2 osteoblast-like cells after cell culture for 24 h in the MMEM preconditioned with

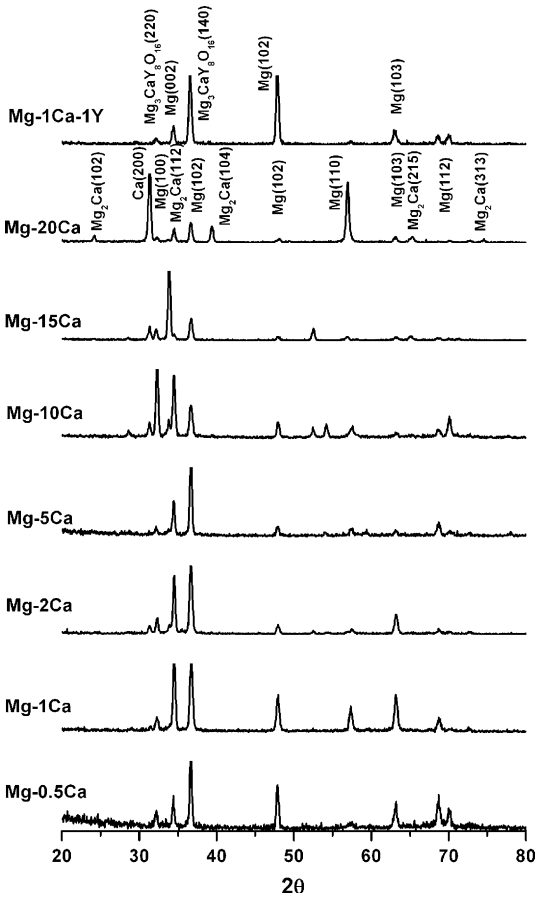

Fig. 3 XRD patterns of the Mg–*x*Ca and Mg–1Ca–1Y alloys

Table 1 Corrosion rate of Mg alloys in MMEM and SBF (μg/mm^2/day)

Alloy sample	Mg–0.5Ca	Mg–1Ca	Mg–2Ca	Mg–1Ca–1Y
MMEM	0.5	4.5	13.0	98.4
SBF	0.4	2.6	10.6	142.7

the Mg–0.5Ca, Mg–1Ca, Mg–2Ca and Mg–1Ca–1Y alloys. The cell viabilities of Mg–0.5Ca, Mg–1Ca and Mg–1Ca–1Y were 89.3, 89.0 and 89.1%, respectively, and were not significantly different ($p > 0.05$) to 91.5% of the control. The number of live and dead cells was similar to that of the control group (Fig. 5). It can be concluded that Mg–0.5Ca, Mg–1Ca and Mg–1Ca–1Y alloys are biocompatible alloys. Compared to the Mg–1Ca alloy, the Mg–1Ca–1Y alloy showed the same level of cell viability and proliferation, which indicates that the Y addition (1 wt%) to the Mg–1Ca alloy does not improve the biocompatibility, nor deteriorate it. The cell viability in the extract of the Mg–2Ca alloy was only 57%, and it was significantly lower than that of the control group ($p > 0.05$). Less live cells were observed in the extract of

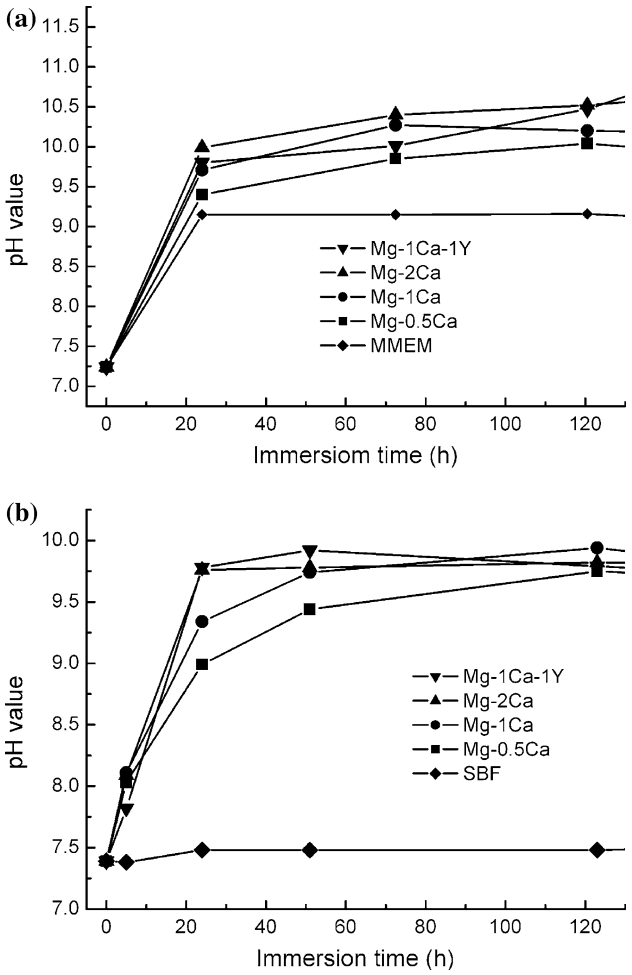

Fig. 4 The pH value of **a** media and **b** SBF with the immersion of the Mg–*x*Ca and Mg–1Ca–1Y alloys

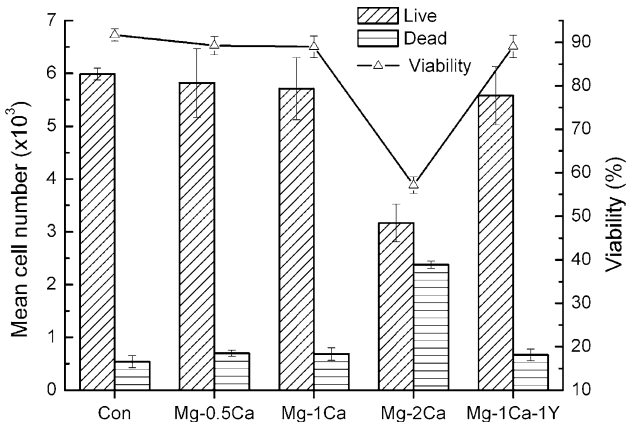

Fig. 5 Cell viability in the extracts of the Mg–*x*Ca and Mg–1Ca–1Y alloys after cell culture for 24 h

the Mg–2Ca alloy, indicating a lower biocompatibility of the Mg–2Ca alloy.

Figure 6 shows the morphologies of SaOS2 osteoblast cells after cell culture for 24 h in the MMEM solution for

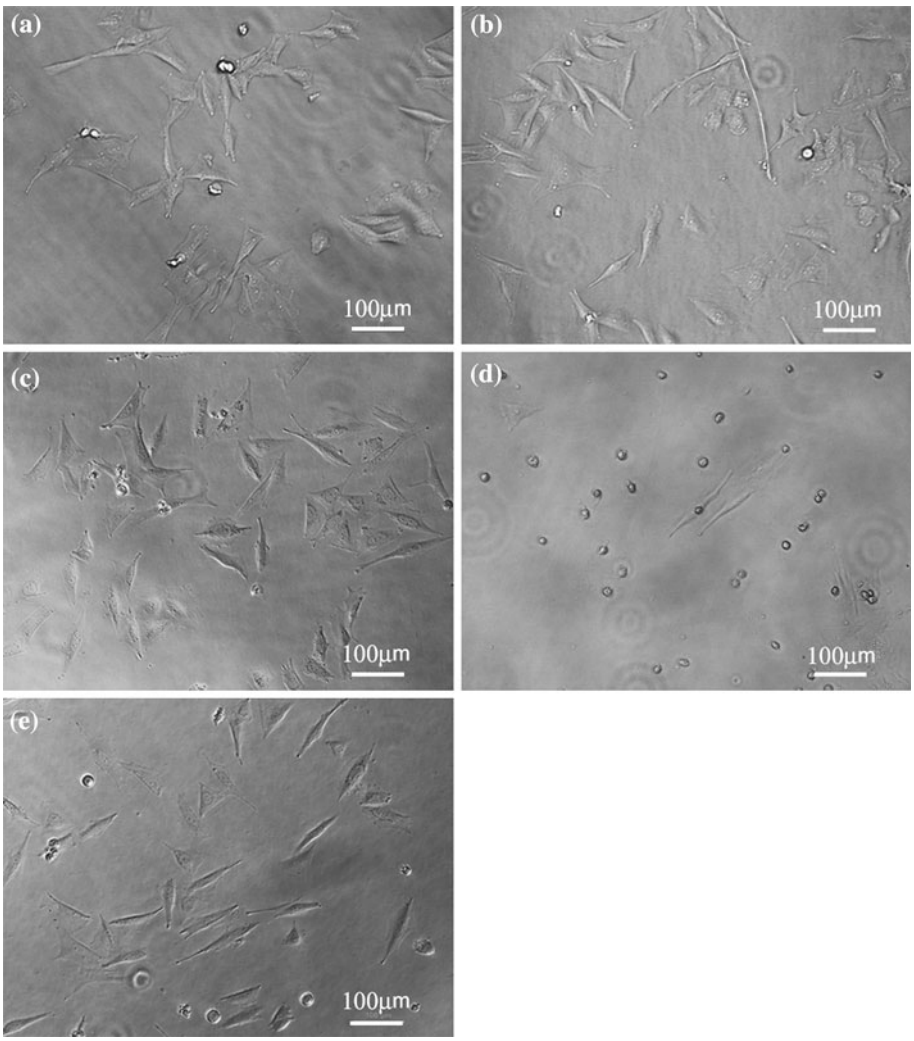

Fig. 6 Cell morphology of **a** the control group and in the extracts of **b** Mg–0.5Ca, **c** Mg–1Ca, **d** Mg–2Ca and **e** Mg–1Ca–1Y alloys after cell culture for 24 h

the control (a) and MMEM preconditioned with the extracts of Mg–0.5Ca (b), Mg–1Ca (c), Mg–2Ca (d) and Mg–1Ca–1Y (e) alloys. As can be seen in Fig. 6a–c and e, cells grew and spread well in the control group and the extracts of the Mg–0.5Ca, Mg–1Ca and Mg–1Ca–1Y alloys, indicating the excellent biocompatibilities of Mg–0.5Ca, Mg–1Ca and Mg–1Ca–1Y alloys. On the other hand, some SaOS2 cells showed a shrinking round shape and spread unwell when cultured in the extract of Mg–2Ca alloy as shown in Fig. 6d), revealing the characteristics of unhealthy cells due to poor biocompatibility. It can be concluded that the Mg–2Ca alloy is less biocompatible than the Mg–0.5Ca, Mg–1Ca and Mg–1Ca–1Y alloys. The results from the cell observation are consistent with the cytotoxicity test results.

Conclusions

In this study, the microstructure, mechanical properties, corrosion behaviour and biocompatibility of Mg–*x*Ca ($x = 0.5$, 1.0, 2.0, 5.0, 10.0, 15.0 and 20.0%) and Mg–1Ca–1Y alloys were investigated for potential biomedical applications. The conclusions are as follows:

1. The compressive strength, elastic modulus and hardness of the Mg–*x*Ca alloys increase, but the ductility, the corrosion rate and the biocompatibility decrease with the increase of the Ca content.
2. The Y addition leads to an increase in the ductility; but a decrease in the compressive strength, hardness, corrosion resistance and biocompatibility of the Mg–1Ca–1Y alloy when compared to the Mg–1Ca alloy.
3. SBF and MMEM solutions with the immersion of the Mg–*x*Ca and Mg–1Ca–1Y alloys show strong alkalisation, which is disadvantageous for new bone formation and should be considered to avoid.
4. Our findings indicate that Mg–*x*Ca alloys with Ca additions less than 1.0 wt% exhibited good biocompatibility, low corrosion rate and appropriate strength and elastic modulus; whilst the Y deteriorates the

corrosion resistance, biocompatibility, mechanical strength and elastic modulus, although it improves the ductility of the Mg–1Ca alloy.

Acknowledgements The authors acknowledge the financial support for this research through the Australia–India Strategic Research Fund (AISRF) BF030031.

References

1. Staiger MP, Pietak AM, Huadmai J, Dias G (2006) Biomaterials 27:1728
2. Witte F (2010) Acta Biomater 6:1680
3. Witte F, Hort N, Vogt C et al (2008) Curr Opin Solid State Mater Sci 12:63
4. Witte F, Ulrich H, Palm C, Willbold E (2007) J Biomed Mater Res 81(A):757
5. Witte F, Ulrich H, Rudert M, Willbold E (2007) J Biomed Mater Res 81(A):748
6. Hartwig A (2001) Mutat Res Fundam Mol Mech Mutagen 475:113
7. Okuma T (2001) Nutrition 17:679
8. Saris N-EL, Mervaala E, Karppanen H, Khawaja JA, Lewenstam A (2000) Clin Chim Acta 294:1
9. Vormann J (2003) Mol Asp Med 24:27
10. Witte F, Kaese V, Haferkamp H et al (2005) Biomaterials 26:3557
11. Zreiqat H, Howlett CR, Zannettino A et al (2002) J Biomed Mater Res A 62:175
12. Wen C, Guan S, Peng L, Ren C, Wang X, Hu Z (2009) Appl Surf Sci 255:6433
13. Wen CE, Mabuchi M, Yamada Y, Shimojima K, Chino Y, Asahina T (2001) Scr Mater 45:1147
14. Wen C, Yamada Y, Shimojima K, Chino Y, Hosokawa H, Mabuchi M (2003) Mater Sci Forum 419–422:1001
15. Currey JD (2006) Bones structure and mechanics. Princeton University Press, New Jersey
16. Wang H, Shi ZM, Yang K (2008) Adv Mater Res 32:207
17. Wang XJ, Li YC, Hodgson PD, Wen CE (2007) Mater Forum 31:56
18. Li YC, Xiong JX, Wong CS, Hodgson PD, Wen CE (2009) Tissue Eng Part A 15:3151
19. Gibson LG, Ashby MF (1997) Cellular solids: structure and properties. Cambridge University Press, Cambridge
20. Denkena B, Lucas A (2007) CIRP Ann Manuf Technol 56:113
21. Hassel T, Bach FW, Golovko A, Krause C (2006) In: Proceedings of the International Symposium Magnesium Technology Global Age, Montreal, QC, Canada, p 359
22. Liang H, Wan YZ, He F et al (2007) Appl Surf Sci 253:3326
23. Qiao L, Gao J, Wang Y, Wang S (2007) Mater Sci Forum 546–549:459
24. López HY, Cortés DA, Escobedo S, Mantovani D (2006) Key Eng Mater 309–311:453
25. Pietak A, Mahoney P, Dias George J, Staiger Mark P (2008) J Mater Sci Mater Med 19:407
26. Hänzi AC, Gerber I, Schinhammer M, Löffler JF, Uggowitzer PJ (2010) Acta Biomater 6:1824
27. Koch C, Scattergood R, Youssef K, Chan E, Zhu Y (2010) J Mater Sci 45:4725. doi:10.1007/s10853-010-4252-7
28. Figueiredo R, Langdon T (2010) J Mater Sci 45:4827. doi:10.1007/s10853-010-4589-y
29. Figueiredo R, Langdon T (2009) J Mater Sci 44:4758. doi:10.1007/s10853-009-3725-z
30. Steinemann SG (1980) In: Winter GD, Leray JL, De Goot K (eds) Evaluation of biomaterials, advances in biomaterials. Wiley, Chichester
31. Okazaki Y, Rao S, Tateishi T, Ito Y (1998) Mater Sci Eng A 243:250
32. Denkena B, Witte F, Podolsky C, Lucas A (2005) In: Proceedings of the 5th euspen International Conference, Montpellier, France, p 233–236
33. Dabah E, Ben-Hamu G, Lisitsyn V, Eliezer D, Shin K (2010) J Mater Sci 45:3007. doi:10.1007/s10853-010-4302-1
34. Aghion E, Levy G (2010) J Mater Sci 45:3096. doi:10.1007/s10853-010-4317-7
35. Yao HB, Li Y, Wee ATS (2003) Electrochim Acta 48:4197
36. Miller PL, Shaw BA, Wendt RG, Moshier WC (1995) Corrosion 51:922
37. He W, Zhang E, Yang K (2010) Mater Sci Eng C 30:167
38. Nayab SN, Jones FH, Olsen I (2007) Biomaterials 28:38
39. ASTM-International (2004) G 31–72 ASTM International, West Conshohocken
40. Wang XJ, Li YC, Lin JG, Hodgson PD, Wen CE (2008) J Mater Res 23:1682
41. International organization for Standardization (1999) ISO 10993-5, ANSI/AAMI, Arlington, VA
42. Kruse PF, Patterson MK (1973) Tissue culture, methods and application. Academic Press, New York
43. Kim JH, Kang NE, Yim CD, Kim BK (2009) Mater Sci Eng A 525:18
44. Li SS, Tang B, Zeng DB (2007) J Alloy Compd 437:317
45. Li P, Tang B, Kandalova EG (2005) Mater Lett 59:671
46. Wang Q, Chen W, Zeng X et al (2001) J Mater Sci 36:3035. doi:10.1023/A:1017927109291
47. Watanabe H, Yamaguchi M, Takigawa Y, Higahshi K (2007) Mater Sci Eng A 454–455:384
48. Hakamada M, Shimizu K, Yamashita T, Watazu A, Saito N, Iwasaki H (2010) J Mater Sci 45:719. doi:10.1007/s10853-009-3990-x